Fault detection and localization in unshielded twisted pair cable based on observability analysis and reflectometry experimental measurements.

Hermine Judith Idellette Som, Vincent Cocquempot, Virginie Degardin

ACCEPTED MANUSCRIPT

Fault detection and localization in unshielded twisted pair cable based on observability analysis and reflectometry experimental measurements.

To cite this article before publication: Hermine Som Idellette Judith *et al* 2023 *Meas. Sci. Technol.* in press https://doi.org/10.1088/1361-6501/ad0069

Fault detection and localization in unshielded twisted pair cable based on observability analysis and reflectometry experimental measurements

Idellette Judith Hermine Som[1], Cocquempot Vincent[2] and Degardin Virginie[3]

[1]University of Douala, National Higher Polytechnic School of Douala, Electrical and Intelligent Systems Department

[2] Univ. Lille, CNRS, Centrale Lille, UMR 9189 - CRIStAL - Centre de Recherche en Informatique Signal et Automatique de Lille, F-59000 Lille, France

[3] Univ. Lille, CNRS, Centrale Lille, Univ. Polytechnique Hauts-de-France, UMR 8520 - IEMN, F-59000 Lille, France

E-mail: idellettesom@yahoo.fr vincent.cocquempot@univ-lille.fr virginie.degardin@univ-lille.fr

Corresponding author: Idellettte Judith Hermine Som idellettesom@yahoo.fr

June 2023

Abstract.

In this paper, an efficient method is proposed for detecting and locating a soft fault, i.e. a physical degradation, in a Y-shaped network of unshielded twisted pair cables. The method uses jointly the observability analysis and time-frequency domain reflectometry experimental measurements. The fault detection consists in checking the consistency between the known characteristics of the cable under no-fault and faulty conditions, with the maximum value of a normalized time-frequency cross-correlation function computed on a sliding time window whose length is equal to the boundary exact observability time. The cable transmission speed and the wired network observability time are combined to locate precisely the fault. Soft faults are artificially created by connecting resistors of different values to the test cable. Experimental results show the efficiency of our fault detection and localization method.

Keywords: Unshielded twisted pair cable, Fault location, Experimental measurements, Joint time-frequency domain reflectometry.

Correspondence to: Electrical and Intelligent Systems Departement, National Higher Polytechnic School of Douala, University of Douala, Cameroon

E-mail address: blackidellettesom@yahoo.fr ORCID: 0000-0001-9600-2649

1. Introduction

Cables are widely used in various industrial and transport sectors, their role is to ensure the transmission of energy or information within a system. Different types of cables are

used depending on the type of signal being transported.

Besides, cables are generally installed in harsh environments, making them prone to degradation or faults such as bad connections or insulation failure and possibly conductor cuts. These faults are divided into two categories, namely soft faults and hard faults, based on their severity and impact on data and energy transmission [1].

A cable degradation changes the electrical parameters of the transmission line. Degradation tends to develop to a hard fault like short circuit or open circuit, which results in total system breakdown. For example, a faulty cable in an aircraft can cause significant malfunctions and consequences, which can be dramatic for the aircraft, the environment, and of course the passengers. Therefore a high availability and reliability of a wired network relies on the capability to detect incipient faults very early.

Different diagnosis methods are used depending on the type of cable, complexity and security constraints of the wired network. The commonly used methods are visual inspection, X-ray, guided ultrasonic waves, infrared thermal imaging. These methods are intrusive and may be destructive [2]. Recently, signal-based methods have been proposed. The principle is to inject a dedicated reference signal in the cable and measure either the characteristics of the transmitted signal [3] or the characteristics of the reflected signal [1]. The latter is known as a reflectometry method. The conventional reflectometry methods can be categorized into time-domain reflectometry (TDR) and frequency-domain reflectometry (FDR) [4], [5], [6]. A review of existing reflectometry-based methods is presented in [1].

To enhance the accuracy in reflectometry, digital signal processing techniques were suggested, for instance the spatial resolution to locate fault in a cable [6], a combined FDR and inverse fast Fourier transform (IFFT) to locate the position of a degradation or abnormality in a polymer-insulated electric cable in [7]. In addition to the aforementioned techniques, time-frequency solutions are also being explored.

The joint time-frequency domain reflectometry (JTFDR) captures many of the advantages of both TDR and FDR by allowing customized reference signal parameters like frequency bandwidth, center frequency, and time duration to provide a unique time-frequency cross-correlation function in order to detect soft faults with acceptable accuracy. JTFDR techniques were applied to monitor high-temperature superconducting cables [8], shielded cable [9], or to study and follow the aging process of electric power cables [10], [11].

This paper proposes an original method to locate faults in a Y-shaped network composed of unshielded twisted pair (UTP) cables. The method is based on observability analysis and JTFDR experimental measurements. The contributions are the following:

- The JTFDR is used to get the nominal reflected signal in healthy conditions (no-fault) by injecting a chirp incident signal multiplied by a Gaussian time envelope with a swept sine wave covering a frequency band of interest.
- The principle of fault detection is to compare, on a sliding time window, the amplitudes of the reflected signal with a predefined threshold. The threshold is fixed

with the maximum value of a normalized time-frequency intercorrelation (NTFI) for a non degraded cable. The length of the sliding time window is the so-called boundary exact observability time, which is equal to the minimum time required to compute the NTFI for the considered network. It should be pointed out that in the existing literature, this NTFI calculation is performed within a limited time interval, without specifying the width of this time window.

- In reflectometry, the reflected signal is collected at the injection point of the incident signal. The observation is thus made from one side of the cable. Using the known cable transmission speed and the wired network architecture (length, configuration), the system observability time defined by [12] is determined and used to locate the fault.
- The local variation of the primary parameters of the cable especially R in the $RLCG$ transmission line model due to a cable fault are artificially created by inserting resistors of different values connected in series to several points along the test cable. Short and open circuits are also tested in the experimental bench.

The remaining of the paper is organized as follows. In Section II, the theoretical background on transmission line models and the reflectometry technique are briefly introduced. Section III focuses on the proposed fault detection and localization schemes. The experimental setup and results on fault diagnosis are discussed in Section IV and finally Section V draws a conclusion.

2. Theoretical background

This section presents the reflectometry principles. First, a preliminary reminder of the transmission line theory is introduced.

2.1. Transmission line theory

A transmission line is modelled by a distributed-parameter transport differential equation, where voltage and current are expressed in magnitude and phase over its length. It is often schematically represented as a two-wire line or a transverse electric magnetic (TEM) wave propagation. Conductors are composed of an infinite series of two-port elementary components, each representing an infinitesimally short segment dz of the transmission line.

Figure 1 represents the equivalent electric circuit of an element dz of the transmission line where

- $v(t,z)$ and $i(t,z)$ are, respectively, the voltage and the current through the transmission line at distance z and time t.
- Rdz is the resistance of the conductors, expressed in Ohm per unit length.
- Ldz is the inductance (due to the magnetic field around the wires, self-inductance), expressed in Henri per unit length.

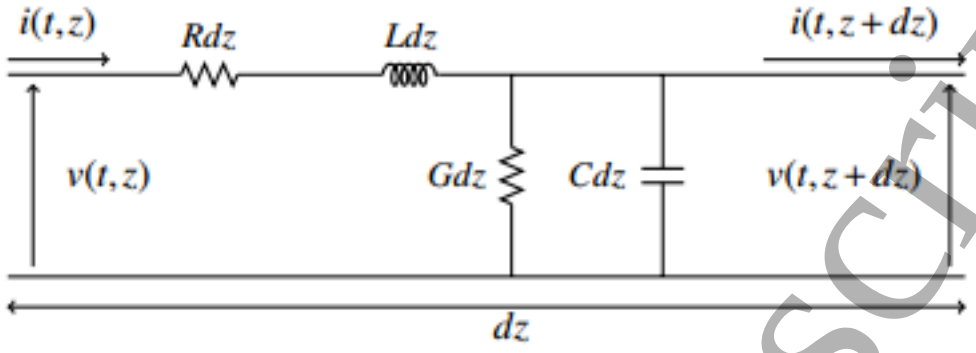

Figure 1: Electric transmission line

- Cdz is the capacitance between the two conductors, represented by a shunt capacitor and expressed in Farad per unit length.
- Gdz is the conductance of the dielectric material separating the two conductors, represented by a shunt resistance and expressed in Siemens per unit length.

Applying Kirchhoff's voltage and current law to the circuit shown in Fig.1, we get

$$\begin{cases} \partial_t i(t,z) + \frac{1}{L(z)}\partial_z v(t,z) + \frac{R(z)}{L(z)} i(t,z) = 0 \\ \\ \partial_t v(t,z) + \frac{1}{C(z)}\partial_z i(t,z) + \frac{G(z)}{C(z)} v(t,z) = 0 \end{cases} \tag{1}$$

(1) is the time-domain form of the so-called *telegrapher equations* on transmission line of length l with the initial condition

$$t = 0: \quad [i(0,z), v(0,z)]^T \triangleq [i^0(z), v^0(z)]^T, \ 0 \le z \le l \tag{2}$$

Consider a transmission line powered by a voltage generator (see Fig.2) which delivers the excitation signal to a load of impedance Z_l

At steady state, the voltage and current take the form of monotonic sinusoidal waves:

$$\begin{cases} i(w,z) = I(w,z)e^{jwt} \\ v(w,z) = V(w,z)e^{jwt} \end{cases} \tag{3}$$

where w is the angular frequency of the steady-state wave. In this case, the telegrapher's equations are reduced to

$$\begin{cases} \frac{d^2 i(w,z)}{dz^2} - \gamma^2 i(w,z) = 0 \\ \\ \frac{d^2 v(w,z)}{dz^2} - \gamma^2 v(w,z) = 0 \end{cases} \tag{4}$$

Solutions of (4) result from the combination of incident waves ($I^+(w,z)$,$V^+(w,z)$) and reflected waves ($I^-(w,z)$,$V^-(w,z)$) propagating along the cable, which leads to the following

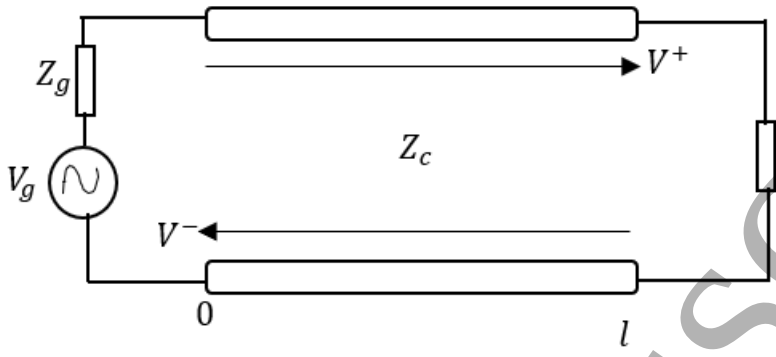

Figure 2: Transmission line powered by a voltage generator and charged by an impedance Z_l

$$\begin{cases} i(w,z) = I^-(w,z)e^{-\gamma z} + I^+(w,z)e^{+\gamma z} \\ v(w,z) = V^-(w,z)e^{-\gamma z} + V^+(w,z)e^{+\gamma z} \end{cases} \tag{5}$$

where $\gamma = \sqrt{(R+jwL)(G+jwC)}$ is the propagation constant, which represents the attenuation and dispersion of the signal along the cable of characteristic impedance $Z_c = \sqrt{\frac{R+jwL}{G+jwC}}$.

2.2. Reflectometry and reflection coefficient

Reflectometry is a high frequency diagnostic method. It is based on a radar-like principle of sending a signal and analyzing the reflected signal. Reflectometry is used in numerous fields owing to its non destructive characteristics. One of the applications is the localization of faults in wired networks.

In fact, as shown in Fig.3, the incident signal is propagated along the line and when it encounters an electrical discontinuity as for instance, impedance variation, fault, shunt [13], a part of the energy is sent back to the injection point and the other part is transferred to the line. In some cases, there is no transmitted wave, all energy is sent back to the injection point.

The reflection coefficient Γ is the ratio between reflected and incident signals

$$\Gamma = \frac{V^-(w,z)e^{-\gamma z}}{V^+(w,z)e^{-\gamma z}} \tag{6}$$

From Fig. 2, (6) yields

$$\Gamma(w,z) = \frac{Z_l - Z_c}{Z_l + Z_c} \tag{7}$$

Indeed, the reflection coefficient is null with an adapted load (i.e, $Z_l = Z_c$).

The reflection coefficient may also be computed from the scattering matrix model with S_{11}-parameter [14].

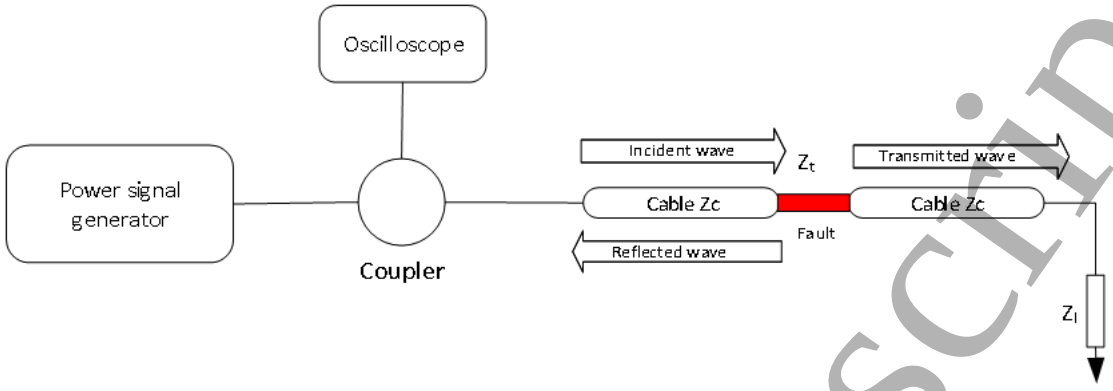

Figure 3: Reflectometry principle

3. Fault detection and localization scheme

The high availability and reliability wired network relies on the efficiency to monitor cable's degradation to prevent total system breakdown. TDR and FDR both give mitigated results to tackle desired performance [1]. To enhance the limitation, several reflectometry techniques have been deployed to diagnose more efficiently and accurately incipient faults on wired network, among them the time-frequency techniques.

The joint time-frequency domain reflectometry (JTFDR) captures many of the advantages of both TDR and FDR by allowing more flexibility and adaptation to the characteristics of the cable to be diagnosed [8]. Features can be adjusted as frequency bandwidth, center frequency, and time duration to provide a unique time-frequency cross-correlation function in order to detect degradation with acceptable accuracy (see for e.g.,[15]).

JTFDR is a three-step process:

1. Injection of a frequency chirp signal, defined to minimize distortion as it propagates through the cable.
2. Measurement of the reflectogram and calculation of its Wigner-Ville transform [16].
3. Application of a normalized time-frequency cross-correlation function, whose peaks correspond to cable discontinuities.

In this work, the JTFDR framework is used to extract signal characteristics (frequency, voltage, shape, position) from measurements. These features are thus compared to *a priori* known characteristics of the UTP cable or the Y-shaped network under no-fault and fault hypotheses.

3.1. Nominal reflected signal

Since the JTFDR considers information both in time and frequency domains at the same time, we use a linearly increasing Gaussian envelope chirp reference signal $g(t)$

as an incident signal which has an adjustable time duration and frequency bandwidth together.

The signal $g(t)$, defined by Eq. 8 is injected at one end point of the Y-shaped network in heathly conditions, to get reference reflected signals which will be used later to build the detection threshold.

$$g(t) = \left(\frac{\alpha}{\pi}\right)^{\frac{1}{4}} .e^{-\alpha t^2/2} \tag{8}$$

It is stated that the reflection coefficient varies according to the impedance discontinuity within the electrical transmission network. The reflected signal presents a succession of peaks correlated to the incident wave reflections at different discontinuities within the cable (faults, nodes and connectors positions).

Let $G(w) = FT\{g(t)\}$ be the Fourier transform of $g(t)$, the reflected signal $S(t)$ is given by :

$$S(t) = \frac{1}{2\pi}\int_{-\infty}^{+\infty} G(w)S_{11}e^{jw\mathcal{T}_f}dw \tag{9}$$

where $\mathcal{T}_f$ is the offset time between the peak of the incident and reflected signals in the cross-correlation.

The S_{11}-parameter is computed by a vector network analyzer (VNA).

3.2. Fault Detection

The general principle of fault detection, described by Fig.4, consists in comparing the amplitudes of reflected signal with a computed threshold.

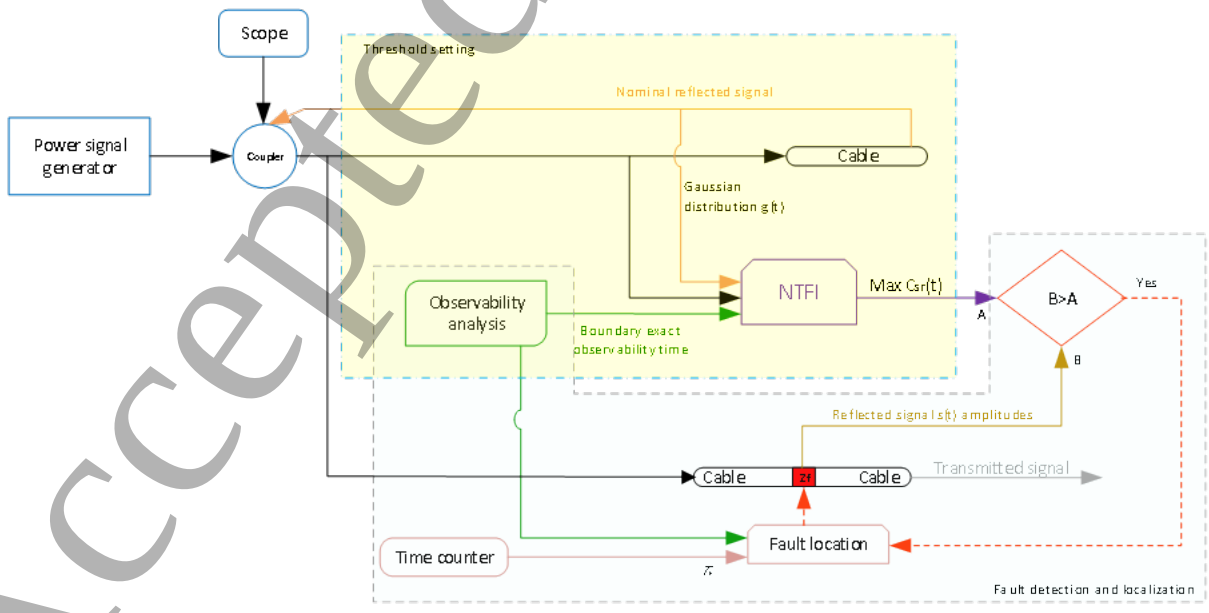

Figure 4: Fault detection and location scheme

Fig.4 highlights the fact that the system observability analysis (One can see that the observability analysis feature is shared between the two blocks) is the key of the two major paper's contributions:

1) The threshold setting is performed off-line by computing the maximun of $C_{sr}(t)$

2) The fault detection and localization scheme is operated online.

The power signal generator, the coupler, and the scope are the firmware parts which function is to generate, collect and visualize the reflectometry incident signal on a healthy cable for threshold setting purpose and on a cable test in order to tune the the fault detection scheme.

Note that in Fig.4, continuous lines represent data flows and the dotted ones, the decision flows.

The principle of fault detection is to compare, on a sliding time window, the amplitudes of the reflected signal with a predefined threshold. The threshold is fixed with the maximum value $C_{sr}(t)$ of a normalized time-frequency intercorrelation (NTFI) for a non degraded cable. The length of the sliding time window is the so-called boundary exact observability time, which is equal to the time required to compute the NTFI for the considered network.

In reflectometry, the reflected signal is collected at the injection point of the incident signal. The observation is thus made from one side of the cable. Using the known cable transmission speed and the wired network architecture (length, configuration), the system observability time defined by [12] is determined and used to locate the fault.

Inspired by [15], the threshold is fixed as the maximum value of the normalized time-frequency inter correlation (NTFI) $C_{sr}(t)$. The NTFI correlates, over a limited time interval, the incident signal $g(t)$ with all the time-delayed versions of the reflected signal $s(t)$.

$$C_{sr}(t) = \frac{2\pi}{E_r(t).E_s} C(t) \tag{10}$$

The terms $E_r(t)$ and E_s are normalization factors, thus, $C_{sr}(t) \in [0;1]\ \forall t$.

$$C(t) = \int_{t'=t-T_s}^{t'=t+T_s} \int_{-\infty}^{+\infty} W_s(t', w) W_g(t'-t, w) dw dt' \tag{11}$$

$$E_r(t) = \int_{t'=t-T_s}^{t'=t+T_s} \int_{-\infty}^{+\infty} W_s(t', w) dw dt' \tag{12}$$

$$E_s = \int_{-\infty}^{+\infty} \int_{-\infty}^{+\infty} W_g(t', w) dw dt' \tag{13}$$

where $W_g(t, w)$ and $W_s(t, w)$ are the Wigner-Ville transform [16] of incident and reflected signals $g(t)$ and $s(t)$ respectively.

T_s is the width of the temporal sliding window to be defined. It should be pointed out that in the existing literature, this NTFI calculation is performed within a limited time interval, without specifying the width of this time window.

Wired networks are transport systems, thus, the incident signal propagates along the network on each transmission line with the speed or transport coefficient λ equals to $\frac{1}{\sqrt{LC}}$ where L and C are respectively the line inductance and capacitance. Obviously, for each transmission line of length l,

$$T_s = \frac{l}{\lambda} = l\sqrt{LC} \tag{14}$$

The NTFI normalises the disparities of the reflected signal due to the non-homogeneity of the cable. The maximum of $C_{sr}(t)$ sets an optimum in terms of admissible reflected signal amplitude. Thus, detecting the maximum of $C_{sr}(t)$, therefore allows us to determine whether a fault is present or not.

3.3. Fault localization

The advantage of NTFI is its ability to detect low amplitudes fault with acceptable accuracy. However, this technique is not efficient to locate precisely a soft fault. To improve fault localization, it was proposed to combine JTFDR with other methods : pattern recognition methods [17], wavelet Transform [18], convolutional neural network [4].

In this paper, we propose to combine JTFDR and observability analysis to locate precisely a fault on a Y-shaped network.

Transport flow networks like water or electrical distribution systems are hyperbolic systems of non-conservative laws [19]. Efficient results on fault detection and isolation have been obtained for such systems, using the observability analysis. A Y-shaped electrical network is an hyperbolic system (based on the *telegraphists' equation*) and the theory developed in a general framework [12] can therefore be applied.

Definition 1 A system is said to be exactly observable in a given domain Ω if and only if the initial state of the system can only be reconstructed by measurements over a finite time interval. The minimum time $\mathcal{T}_o > 0$ is the so-called observability time.

Transport flow systems are modelled by the following general equations

$$\begin{cases} \partial_t W(t,z) + S(z)\partial_z W(t,z) + H(z)\, W(t,z) = 0 \\ W(0,z) = W^0(z) \end{cases} \tag{15}$$

where $W(t,z)$ are unknown transported variables or densities.

Remark 1 Equations (1)-(2) are under the form (15) with

$$W(t,z) = \begin{bmatrix} i(t,z) \\ v(t,z) \end{bmatrix} \quad S(z) = \begin{bmatrix} 0 & \frac{1}{C(z)} \\ \frac{1}{L(z)} & 0 \end{bmatrix} \quad H(z) = \begin{bmatrix} \frac{R(z)}{L(z)} & 0 \\ 0 & \frac{G(z)}{C(z)} \end{bmatrix} \tag{16}$$

thus, a transmission line is indeed a kind of transport flow system.

The exact observability of transport flow systems (15) can be stated at one side or at both sides of the system's boundaries. In reflectometry, the reflected signal is collected at the injection point of the incident signal. The observation is thus made at one side of the system.

Besides, it is commonly stated that the reflection coefficient varies according to the impedance discontinuity within the electrical transmission network. The reflectogram presents a succession of peaks correlated to the incident wave reflections at different discontinuities within the network (fault in the lines, positions of the nodes, and connectors). Therefore, to locate the impedance discontinuities, the propagation speed along the wired network and the exact observability time may be used.

Lemma 1 *One side boundary observation of a single cable [12].*
Consider an electric transmission line represented in Fig.1 and described by (1)-(2). Let $\mathcal{T}$ *be a number verifying*

$$\mathcal{T} > 2l\sqrt{LC} \tag{17}$$

Suppose that $[v(t,0), i(t,l)]^T \equiv (0,0)^T$. *For any initial condition (2), such that the norm* $\|[i^0(z), v^0(z)]^T\|_{\mathcal{C}^1[\ 0,l]}$ *is sufficiently small and the compatibility conditions* $\mathcal{C}^1$ *with (1) are satisfied at the points* $(t,z) = (0,0)$ *and* $(t,z) = (0,l)$ *respectively, if the values* $v(t,0)$ *at* $z = 0$ *are observed on the interval* $[\ 0, \mathcal{T}]$, *then the initial data* $[i^0(z), v^0(z)]^T$ *are uniquely determined and the following inequality is verified:*

$$\| \left[i^0(z), v^0(z)\right]^T \|_{\mathcal{C}^1[0,l]} \leq \| \ v(t,0)\|_{\mathcal{C}^1[0,\mathcal{T}]} \tag{18}$$

The generalization of Lemma 1 to a Y-shaped network is given by the following lemma.

Lemma 2 *One side boundary observation of a* Y*-shaped network with* m *incoming and* $n-1$ *outgoing flows [12].*

Let $n = 3$, $m = 1$ *and* $\mathcal{T}$ *be a number verifying*

$$\mathcal{T} > 2l_m\sqrt{LC} + \max_{\jmath=m+1,\dots,n} 2l_\jmath\sqrt{LC} \tag{19}$$

Suppose that $[v_\iota(t,0), i_\jmath(t,l_\jmath)]^T \equiv (0,0)^T, \forall \jmath = 1,...,n$. *For any initial condition (2),* $\forall \jmath = 1,...,n$ *, such that the norm* $\|[i^0_\jmath(z), v^0_\jmath(z)]^T\|_{\mathcal{C}^1[\ 0,l_\jmath]}$ *is sufficiently small and the compatibility conditions* $\mathcal{C}^1$ *with piece-wise (1) are satisfied at the points* $(t,z) = (0,0)$ *and* $(t,z) = (0,l_\jmath)$ *respectively, if the values* $v_\jmath(t,0)$ *at* $z = 0 \forall \jmath = 1,...,n$ *are observed on the interval* $[\ 0, \mathcal{T}]$, *then the initial data* $[i^0_\jmath(z), v^0_\jmath(z)]^T$ *are uniquely determined and the following inequality is verified:*

$$\sum_{\jmath=1}^{n} \| \left[i^0_\jmath(z), v^0_\jmath(z)\right]^T \|_{\mathcal{C}^1[0,l_\jmath]} \leq \sum_{\jmath=m+1}^{n} \| \ v_\jmath(t,0)\|_{\mathcal{C}^1[0,\mathcal{T}]} \tag{20}$$

Based on the aforementioned Lemmas, the boundary exact observability time $\mathcal{T}_o$ is set at the limit of (17) and (19) depending of the network configuration.

On a single cable

$$\mathcal{T}_o = 2l\sqrt{LC} \tag{21}$$

On Y-shaped network $n = 3$, $m = 1$

$$\mathcal{T}_o = 2l_m\sqrt{LC} + \max_{\jmath=m+1,\dots,n} 2l_\jmath\sqrt{LC} \tag{22}$$

Going back to (10)-(14), it obviously appears that the NTFI is computed on the sliding time window $[t - T_s, t + T_s]$ which length is equal to $2T_s$ i.e the boundary exact observability time $\mathcal{T}_o = 2T_s$. Thus, observing the reflected signal at the same point of the injected incident signal (reflectometry principle), one can update the state of the wired network and get the fault location z_f.

Recalling the boundary exact observability time defined in Lemmas 1 and 2, a fault located at the curvilinear coordinate $z_f \in [0, l_\jmath]$, $\jmath = 1, ..., n$, is uniquely localize from the reflected signal measurements collected during an interval $[0, \mathcal{T}_f]$. $\mathcal{T}_f$, the offset time between the peak of the incident and reflected signals in the cross-correlation.

On a Y-shaped network where $n = 3$ and $m = 1$, the fault localization is performed in two steps: identification of the faulty branch and location of fault on the faulty branch:

- The fault is located on the incoming flow branch m at z_f, $\mathcal{T}_f < 2l_m\sqrt{LC}$

$$z_f = \frac{1}{2\sqrt{LC}} \times \mathcal{T}_f \tag{23}$$

- The fault is located on a specific outgoing flow branch $m + 1, ..., n$ at z_f $\mathcal{T}_f > 2l_m\sqrt{LC}$

$$z_f = \frac{1}{2\sqrt{LC}} \times \mathcal{T}_f - l_m \tag{24}$$

4. Experimental setup and results

4.1. Test bench description

A test bench, shown in Fig.5, has been set up to test the efficiency of the proposed fault detection and localization method. The test bench is a Y-shaped network (see Fig.6), where three branches are connected with a node. The installed cables are aeronautic DRB18-type cables with a characteristic impedance $Z_c = 120\Omega$.

A DRB18 cable is an unshielded twisted pair cable designed for aircraft [20] with point-to-point or bus topology, using a carrier sense multiple access/collision detection (CSMA/CD) baseband communication protocol. The parameters of the test cable are given in table 1.

The $NSA937901$ $M1606$ module [21], designed specifically for aircraft, is used to connect the three branches of the Y-network. Each cable termination is equipped with a balun to connect the VNA two-wire cable.

Figure 5: Laboratory test bench

Table 1: Definition and values of cable parameters.

Parameter	Value
Frequency (f)	$[0.25 : 100]$ MHz
Conductor diameter (d)	1.12×10^{-3} m
Distance between conductors (D)	2.11×10^{-3} m
Copper conductivity (σ)	$5,8 \times 10^{7}$ S/m
Vacuum permeability (μ_0)	4×10^{-7} H/m
Dielectric loss tangent $\tan(\delta)$	$2,83 \times 10^{-2}$
Dielectric permittivity (e)	1.377×10^{-11}
Corrective term : (η)	$1 \leq \eta \leq 1.3$ ($\eta = 1$)

Connectors $C_1, ..., C_5$ are used to connect, in series or in parallel, resistors of different values to the healthy $DRB18$ cable to emulate faults.

Fig.7 shows the measurement chain with different components.

4.2. Fault detection and localization: Experimental results

The test bench is built to be easily manipulated for fault diagnosis purpose. The AD-branch may be disconnected from the network to study a single cable. A fault represented by an impedance $Z_f \in \{5\Omega;\ 50\Omega;\ 500\Omega;\ 5K\Omega\}$ can be inserted in series or

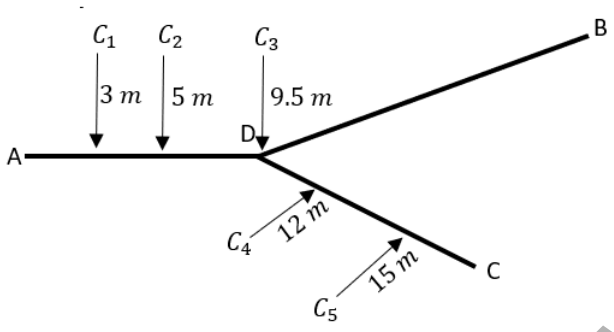

Figure 6: Network topology and location of connectors

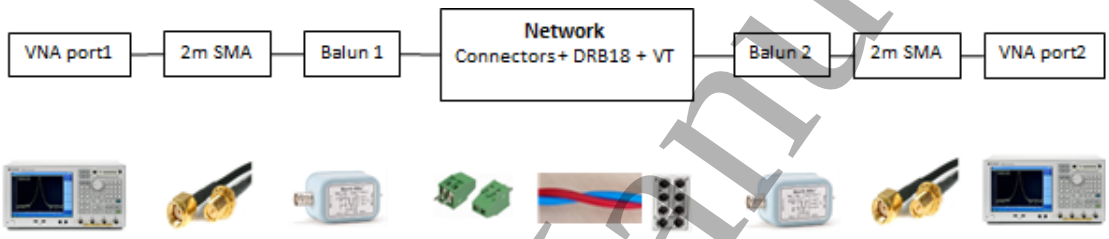

Figure 7: Measurement chain

in parallel and removed in two different positions. The length of the branches AD, DC and DB are respectively $l_1 = 9.5$ m , $l_2 = 9.5$ m and $l_3 = 12$ m. The distance between the fault positions and the node A for AD-branch and D in DC-branch is $z_f = 4.3$ m. Our goals is to show the validity of diagnosis method's.

Firstly, experiments are conducted on the non-faulty Y-shaped network and disconnected AD-branch. Recorded measurements are kept as nominal reflected signals in order to compute the maximum value of the normalized time-frequency inter correlations, $C_{sr}(t)$.

Secondly, hard faults (short and open-circuits) and soft faults (degradations) are emulated by local variation of the primary parameters especially R in the $RLCG$ transmission line model on the Y-shaped network and on its disconnected AD-branch.

Nominal reflected signal

The vector network analyser (VNA $E5071C$) is used to inject a signal into the network and to measure the transmission coefficients between each source and each two end lines in the frequency band of $[0.25 : 100]$ MHz. The measurements are transmitted to a computer for data processing via MATLAB®. Gaussian noise with a signal to noise ratio of 100 dB is added via MATLAB® to get the reflected signal in a realistic environment for an embedded system.

In healthy conditions (no-fault), reflected signals of the Y-shaped network and of the disconnected AD-branch are collected at the injection point of the Gaussian envelope chirp incident signal. They are represented in Fig.8.

The observed reflections are due to the non-homogeneity of the UTP cable. High

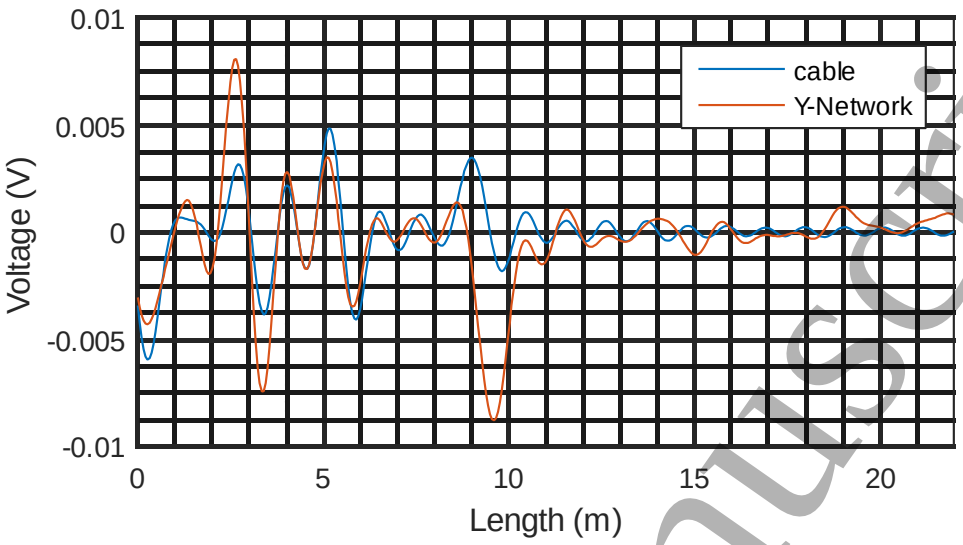

Figure 8: Nominal reflected signal of Y-shaped network and of the disconnected AD-branch (no-fault case)

amplitudes are located around connectors $C_1, ..., C_5$ (see Fig.6).

The MATLAB® function $wvd(x, f_s)$ is used to compute the Wigner-Ville transform of the signals.

For a $DRB18$ cable, $L = 4.98 \times 10^{-7}$ H and $C = 3.47 \times 10^{-11}$ F, which leads to the propagation speed $\lambda \approx 2.41 \times 10^8$ m/s.

By applying (11)-(13), the NTFI is computed on a sliding time of length equal to the corresponding boundary exact observability time with $T_s = 8.94 \times 10^{-8}$ seconds and $T_s = 3.95 \times 10^{-8}$ seconds respectively for Y-shaped network and the disconnected AD-branch.

The threshold is set at the maximum value of $C_{sr}(t)$ (10). The obtained thresholds are 25×10^{-4} V and 87.5×10^{-4} V respectively for the Y-shaped network and the disconnected AD-branch.

Short circuit (two terminals are externally connected with no resistance) and open circuits (two terminals are externally disconnected) are created in the Y-shaped network and the disconnected AD-branch as described in Fig.9).

The offset time between the peak of the incident and reflected signals in the cross-correlation $\mathcal{T}_f$ is respectively 11.54×10^{-8} seconds and 3.49×10^{-8} seconds for the Y-shaped network and the AD-branch. Using the one-side boundary exact observability, the fault locations are estimated through (24) and (23) at 13.88 m and 4.20 m from A. Compared to real positions, fault location estimation errors are $+0.08$ m and -0.09 m respectively for the Y-shaped network and AD-branch.

Recorded signals with short and open circuits are represented in Fig.10.

Soft faults are now created artificially by inserting an impedance $Z_f \in \{5\Omega;\ 50\Omega;\ 500\Omega;\ 5k\Omega\}$ in series in the same locations as the previous hard faults (see

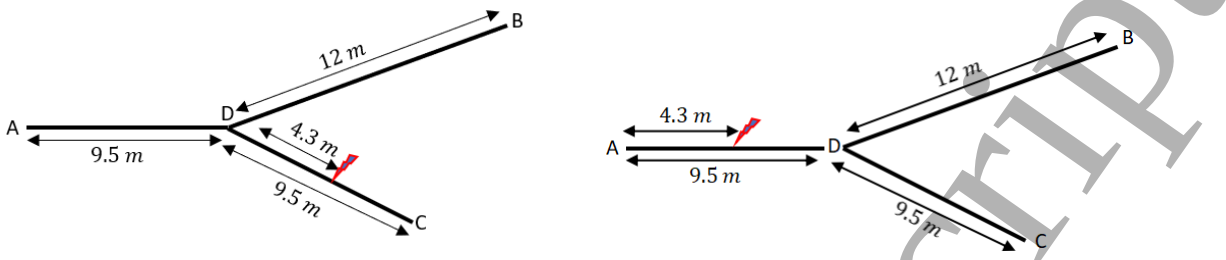

(a) (b)

Figure 9: Hard faults location on the Y-shaped network (a) and the disconnected AD-branch (b)

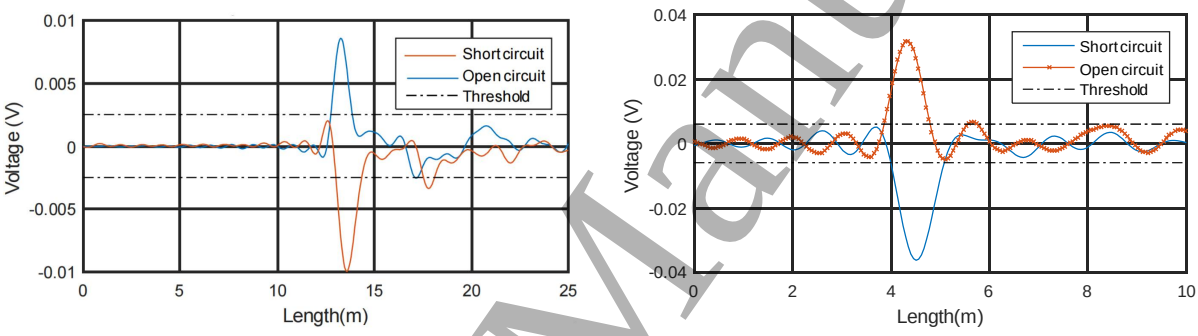

(a) (b)

Figure 10: Recorded signals with short and open circuits on the Y-shaped network (a) and the disconnected AD-branch (b)

Fig.9).

Fig.11 show the effectiveness of the proposed approach to different fault severities.

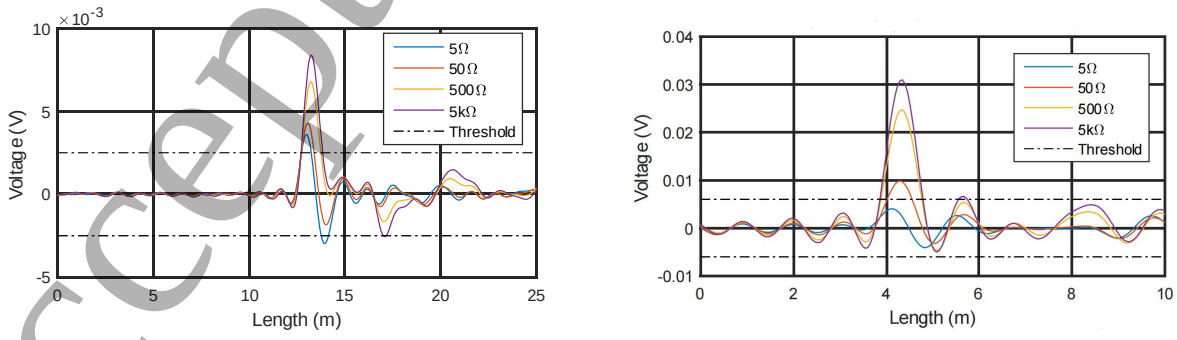

(a) (b)

Figure 11: Recorded signals with resistors connected in series on the Y-shaped network (a) and the AD-branch (b)

Soft faults corresponding to resistors inserted in series produce positive peaks. It

corresponds to the energy dissipation within the cable.

The used detection thresholds ensure the detectability of a series resistance greater than 5Ω which represents 0.5% of cable's nominal characteristic impedance. The peak corresponds to a relative errors of 0.36% to the fault location at 13.75 m from A.

5. Conclusion

A fault detection and localization scheme in a Y-shaped network of unshielded twisted pair cables has been proposed. The principle of fault detection is to compare, on a sliding time window, the amplitudes of the reflected signal with a predefined threshold. The threshold is fixed with the maximum value of a normalized time-frequency intercorrelation (NTFI) for a non degraded cable. The length of the sliding time window is the so-called boundary exact observability time, which is equal to the minimum time required to compute the NTFI for the considered network. The observability time is computed from the network characteristics and parameters. The cable transmission speed and the wired network observability time are combined to locate the fault.

The experimental test bench was built to be easily manipulated for fault diagnosis purpose. Different fault severities were inserted in series in two different positions. Experimental results confirms the efficiency of the proposed fault diagnosis scheme. As future work, we plan to extend the proposed fault diagnosis method to other wired network configurations.

Acknowledgments

The authors would like to thank DIACA project (CPER ELSAT 2020) and Region Hauts-de-France which have supported this work.

References

[1] Furse C. M., Kafal M., Razzaghi R. and Shin Y.-J. Fault diagnosis for electrical systems and power networks: A review. *IEEE Sensors Journal*, vol. 21, no. 2, pp. 888–906, 2020.

[2] Nobile P. A. and Laplatney C. A. Field testing of cables: Theory and practice. *IEEE transactions on industry applications*, vol. 5, pp. 786–795, 1987.

[3] Abdel Karim A.K., Atoui A., Degardin V., Laly P.and Cocquempot V. Bus network decomposition for fault detection and isolation through power line communication, *ISA Transactions*, vol. 137, pp. 492-505, 2023.

[4] Chang S. J. and Park J. B. Wire Mismatch Detection Using a Convolutional Neural Network and Fault Localization Based on Time–Frequency-Domain Reflectometry. *IEEE Transactions on Industrial Electronics*, vol. 66, no. 3, pp. 2102-2110, 2019.

[5] De Paulis F., Boudjefdjouf H., Bouchekara H. R., Orlandi A., Smail M. K. Performance improvements of wire fault diagnosis approach based on time-domain reflectometry. *IET Science, Measurement Technology*, vol. 11, no. 5, pp. 538–544, 2017.

[6] Ohki Y. and Hirai N. Spatial Resolution between Two Abnormalities in a Cable by Frequency Domain Reflectometry. *IEEJ Transactions on Electrical and Electronic Engineering*, vol.16, no.6, pp.822-826, 2021.

[7] Ohki Y. and Hirai N. Location attempt of a degraded portion in a long polymer-insulated cable. *IEEE Transactions on Dielectrics and Electrical Insulation*, vol.25, no.6, pp.2461-2466, 2018.

[8] Wang J., Stone P.E.C., Coats D., Shin Y-J. and Dougal R. A. Health Monitoring of Power Cable via Joint Time-Frequency Domain Reflectometry. *IEEE Transactions on Instrumentation and Measurement*, vol. 60, no. 3, pp. 1047-1053, 2011.

[9] Hua X., Wang L. and Zhang Y. Analysis and diagnosis of shielded cable faults based on finite-element method and time-reversal time-frequency domain Reflectometry. *IEEE Transactions on Industrial Electronics*, vol. 69, no. 4, pp. 4205-4214, 2022.

[10] Lee H. M., Lee G. S., Kwon G.Y., Bang S. S. and Shin Y.J.. Industrial Applications of Cable Diagnostics and Monitoring Cables via Time–Frequency Domain Reflectometry. *IEEE Sensors Journal*, vol.21, no.2, pp. 1082-1091, 2021.

[11] Wang J., Stone P.E.C, Shin Y.J. and Dougal R. A. Application of joint time–frequency domain reflectometry for electric power cable diagnostics. *IET Signal Processing* , Vol.4, no.4, pp.395-405, 2010

[12] Idellette Judith H. S. Synthèse d'observateurs à dérivées partielles pour le diagnostic de défauts des systèmes de distribution de flux. *Thesis, University of Lille 1*, France, 2017.

[13] Sommervogel L. Various models for faults in transmission lines and their detection using time domain reflectometry. *Progress In Electromagnetics Research C*, vol. 103, pp. 123-135, 2020.

[14] Zhang Q., Sorine M. and Admane M. Inverse scattering for soft fault, diagnosis in electric transmission lines. *IEEE Transactions on Antennas and Propagation*, vol. 59, no. 1, pp. 141-148, 2011.

[15] Franchet M., Ravot N. and Picon O. The use of the Pseudo Wigner Ville Transform for detecting soft defects in electric cables. In IEEE/ASME International Conference on Advanced Intelligent Mechatronics (AIM), Budapest, Hungary, 2011, pp. 309-314.

[16] Debnath, L. and Shah, F.A. The Wigner–Ville Distribution and Time–Frequency Signal Analysis. In Wavelet Transforms and Their Applications, Birkhäuser, Boston, MA, pp. 287-336, 2015.

[17] Amloune A., Houssem R. E. H. Bouchekara H. R., Smail M. K., de Paulis F., Orlandi A., Boudjefdjouf H. and Kaikaa M. Y. An intelligent wire fault diagnosis approach using time domain reflectometry and pattern recognition network. *Nondestructive Testing and Evaluation*, vol. 34, no. 1, pp. 99-116, 2019.

[18] Zhang J., Zhang Y. and Guan Y. Analysis of Time-Domain Reflectometry Combined With Wavelet Transform for Fault Detection in Aircraft Shielded Cables. *IEEE Sensors Journal*, vol. 16, no. 11, pp. 4579-4586, 2016.

[19] Gosse L. A well-balanced scheme using non-conservative products designed for hyperbolic systems of conservation laws with source terms. *Mathematical Models and Methods in Applied Sciences*, vol. 11, no. 02, pp. 339-365, 2001.

[20] https://www.prysmiangroup.com/sites/default/files Consulted on may 2023.

[21] https://www.amphenol-airlb.de/files/media/pdf/kataloge Consulted on may 2023.